A Novel Four-Point Bend Test for Strength Measurement of Optical Fibers and Thin Beams—Part II: Statistical Analysis

M. John Matthewson and Gregory J. Nelson

Abstract—**In the first part of this work, a novel implementation of the well-known four-point bend test is described that determines the strength of thin beams and optical fibers by measuring the loading pin displacement, rather than the applied load. This paper extends the analysis of the nonlinear bending behavior to account for the stochastic nature of strength. A statistical analysis is presented that determines the effective tested length in bending and the tension to bending strength ratio. Results are given for both surface and volume flaws as well as for specimens of both circular and rectangular section. Strength measurements on a deliberately weakened silica optical fiber are consistent with the predictions of the analysis.**

I. Introduction

In the first part of this work [1], a novel implementation of the four-point bend test was described which uses the displacement of the loading pins, rather than the applied load, to characterize the specimen strength. The technique is particularly useful for determining the strength of thin, compliant beams and has proved useful for testing relatively weak (compared to pristine silica) optical fibers of various compositions [2], [3], [4]. The principal advantages of the technique are its ease of use, the ability to test several specimens at once, the simplicity of immersing the specimens in a variety of test environments, and the ability to test fibers that are too weak to be tested in two-point bending. The large deflection of the specimen means that the linear beam bending theory that is normally applied to four-point bending is invalid and a detailed nonlinear theory for the fiber stress as a function of deflection was presented. The effect of specimen/pin friction was accounted for and a simple technique was described for making *in situ* measurements of the friction.

The strength of ceramics in general, and optical fibers in particular, is a stochastic variable due to the presence of flaws that are distributed in severity, orientation, and position. This leads to a dependence of the strength on the specimen size since larger specimens are more likely to contain larger flaws and are therefore weaker than smaller specimens. For this reason, strength results obtained using different techniques cannot be directly compared because the specimen sizes will usually be different. We therefore present a statistical analysis for the nonlinear four-point bend test so that its results can be compared to those of tensile and two-point bending, as well as to the linear analysis.

Manuscript received June 5, 1995; revised December 1, 1995. This work was supported in part by the Fiber Optic Materials Research Program at Rutgers University and in part by the New Jersey Commission on Science and Technology.

M. J. Matthewson is with the Fiber Optics Materials Research Program, the Department of Ceramic Science and Engineering, Rutgers University, Piscataway, NJ 08855 USA.

G. J. Nelson is with the Philips Lighting Company, Bath, NY 14810 USA.

Publisher Item Identifier S 0733-8724(96)02952-0.

II. Statistical Analysis

The risk function $f(\sigma)$ is defined by $f(\sigma)\,d\tau$ being the probability that an element of space, $d\tau$, fails by a stress σ. Weakest link theory shows that the cumulative probability of failure by a representative stress σ', $F(\sigma')$, is given by

$$F(\sigma') = 1 - \exp\left(-\int_{\tau} f(\sigma)d\tau\right) = 1 - \exp(-\Re). \quad (1)$$

σ' represents the intensity of the stress field and would be the uniaxial tension for a tensile test or the peak uniaxial stress at the tip of the bend for a two-point bend test. $\Re$ will be called the "risk integral." The integration is over the complete space, τ, containing flaws; $d\tau$ represents an element of surface area of the fiber if surface flaws dominate (as is usually the case for optical fiber) or an element of volume if volume flaws dominate (as would be the case for porous glass fiber or polycrystalline fiber). For convenience, the analysis will be developed assuming surface flaws only and then equivalent results for volume flaws will be shown. Similarly the results will be determined for fibers with circular cross-section, but results will also be studied for rectangular sections.

In general, σ is a function of position $\sigma(\mathbf{r})$, and hence, $f(\sigma)$ must be integrated over the entire surface of the specimen in order to evaluate $F(\sigma')$. Since the form of $f(\sigma)$ is not known *a priori*, the well-known Weibull distribution is used for its convenience and mathematical simplicity

$$f(\sigma)dA = \left(\frac{\sigma(\mathbf{r})}{\sigma_0}\right)^m \frac{dA}{A_0}. \quad (2)$$

m, the Weibull modulus, is an inverse measure of the width of the distribution. The factor A_0 is a reference area of value unity in the current system of units which ensures that the dimensions of σ_0, which is a measure of the central tendency, are those of stress [5]. Fig. 1 shows a section through the bent fiber from which it may be shown that

$$\sigma(\mathbf{r}) = \sigma(\theta,\phi) = \sigma(\theta)\sin\phi = \frac{Er\sin\phi}{R(\theta)} \quad (3)$$

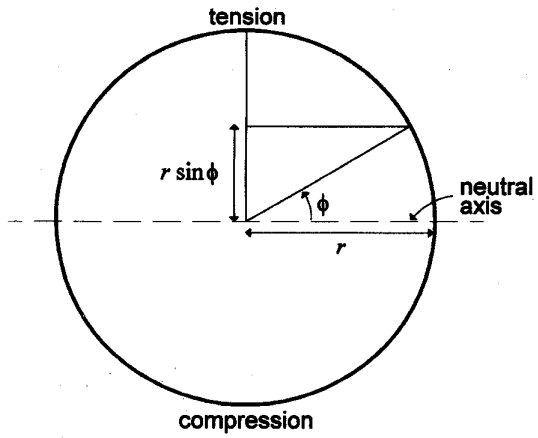

Fig. 1. Section through the bent fiber.

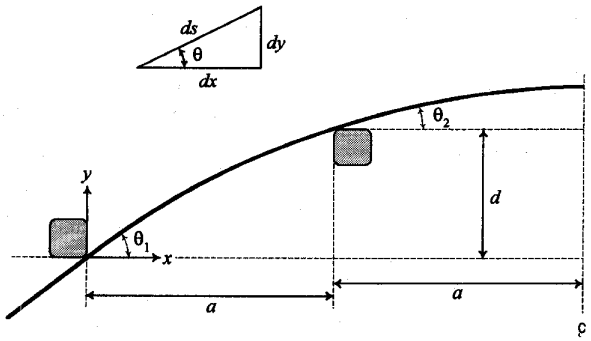

Fig. 2. Schematic defining the geometry of the fiber between the support and loading pins.

where E is Young's modulus, $\sigma(\theta)$ is the stress profile along the maximum tensile surface of the fiber ($\phi = 90°$), $R(\theta)$ is the radius of curvature profile and θ is the angle the fiber makes with the horizontal (Fig. 2) and is a measure of position along the fiber length. The element of surface area, dA, is given by

$$dA = rd\phi ds = \frac{rd\phi\, dx}{\cos\theta} \tag{4}$$

where ds is an element of fiber length and dx is an element of distance between the pins, as defined in Fig. 2. In the case of four-point bending, the integral in (1) becomes

$$\Re_4 = \int_A f(\sigma)dA = \int_{x=0}^{4a}\int_{\phi=0}^{\pi}\left(\frac{Er\sin\phi}{R\sigma_0}\right)^m \frac{rd\phi\, dx}{A_0\cos\theta} \tag{5}$$

$$= \frac{E^m r^{m+1}}{A_0\sigma_0^m}\int_0^{\pi}\sin^m\phi d\phi\int_0^{4a}\frac{dx}{R^m\cos\theta} \tag{6}$$

$$= \frac{2E^m r^{m+1}}{A_0\sigma_0^m}G(m)\int_0^{4a}\frac{dx}{R^m\cos\theta} \tag{7}$$

where

$$G(m)\int_0^{\pi/2}\sin^m\phi d\phi = \frac{\sqrt{\pi}}{2}\frac{\Gamma\left(\frac{m+1}{2}\right)}{\Gamma\left(\frac{m+2}{2}\right)} \tag{8}$$

and $\Gamma(x)$ is the gamma function [6]. The function $G(m)$ is shown in Fig. 3. The integration over ϕ in (5) is only over the tensile surface of the fiber. It is noted that the factor before

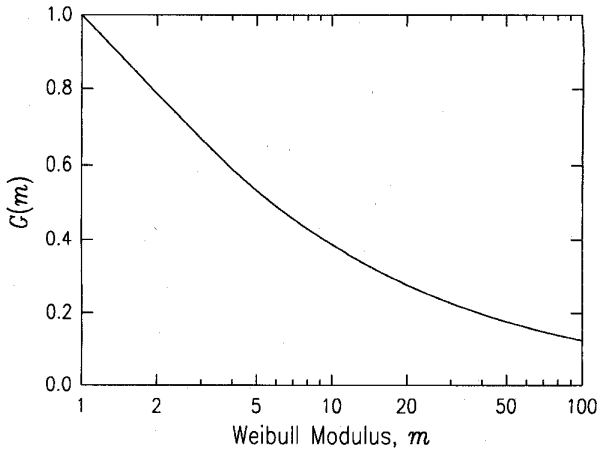

Fig. 3. The dependence of the function $G(m)$ on the Weibull modulus m.

the integration in (7) is a constant for a given fiber that is independent of the geometry of the bend. It is further noted that the integral in (7) is neither constant for a constant applied load (as is the case for uniaxial tension) nor simply scales with the size of the bend (as is the case for two-point bending, [7]) due to the nonlinear nature of the deflection. This means that the integration does not simplify to a simple power of a parameter describing the magnitude of the deflection, such as d. This, in turn, means that the strength distribution is no longer Weibull. However, the deviation from Weibull is small and is not likely to be detectable experimentally. The integral cannot be calculated analytically and is therefore evaluated numerically using the trapezoidal rule at the same time as calculations are made of the curvature profile, $1/R(x)$, in the numerical program described in part I of this work [1].

If the linear bending theory is assumed, the integration in (7) can be performed analytically since, in this case,

$$\frac{1}{R} = \frac{3xd}{4a^3} \qquad 0 \le x \le a \tag{9}$$

$$\frac{1}{R} = \frac{3d}{4a^2} \qquad a \le x \le 2a \tag{10}$$

and $\cos\theta = 1$, giving the result

$$\Re_4' = \left(\frac{3Erd}{4a^2\sigma_0}\right)^m \frac{4ar}{A_0}\frac{(m+2)}{(m+1)}G(m) \tag{11}$$

where the prime represents predictions of the linear bending theory.

The equivalent analysis for a tensile specimen of length l, subjected to a stress σ, gives the risk integral, $\Re_t$

$$\Re_t = \left(\frac{\sigma}{\sigma_0}\right)^m \frac{2\pi rl}{A_0} \tag{12}$$

while the equivalent analysis for two-point bending [7] gives

$$\Re_2 = \frac{4Er^2}{A_0\sigma_{\max}}G\left(\frac{m-1}{2}\right)G(m)\left(\frac{\sigma_{\max}}{\sigma_0}\right)^m \tag{13}$$

where $\sigma_{\max}$ is the maximum tensile stress at the tip of the bend and is given by

$$\sigma_{\max} = \frac{2.396Er}{D} \tag{14}$$

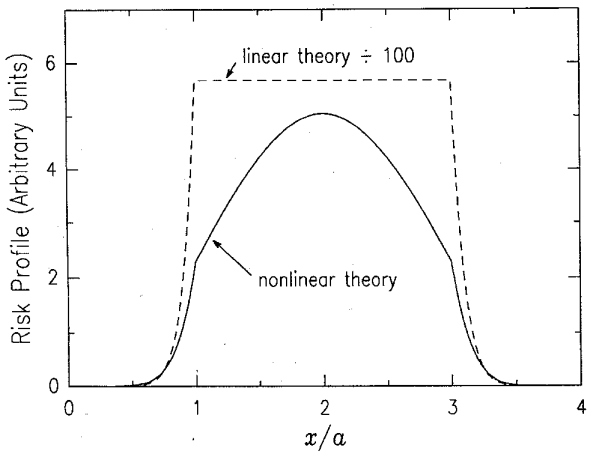

Fig. 4. Risk profile along the fiber calculated for $d/a = 1.26$ ($\theta_1 = 60°$), $m = 10$ and $\mu = 0$. Note the linear theory has been scaled by a factor of 0.01.

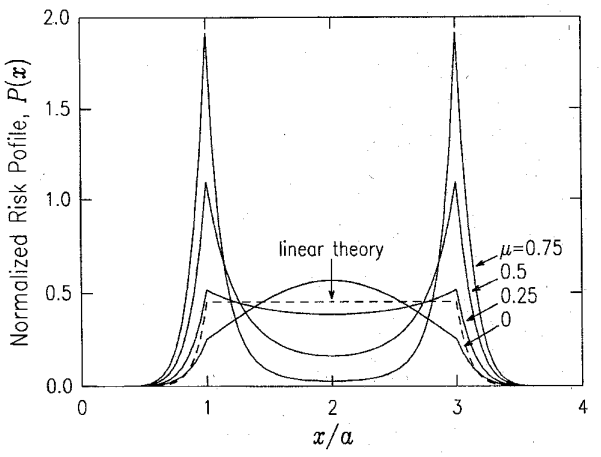

Fig. 5. Normalized risk profile along the fiber calculated for $d/a = 1.26$, $m = 10$ and various values of the pin/fiber friction, μ.

where D is the distance between the neutral axes of the two parallel arms of the bent fiber.

A. Distribution of Failure Origins

The risk function, $f(\sigma)$, may be normalized to unity by dividing by the risk integral $\Re$ forming the distribution along the fiber

$$P(x) = \frac{f(\sigma(x))}{\Re}. \tag{15}$$

For linear test methods, such as uniaxial tension and linear four-point bending, the length of specimen under test does not change during loading. Additionally, increased loading only changes the magnitude of $\sigma(x)$, not its shape. Under these two specific conditions, the magnitude of the applied stress cancels in (15) so that $P(x)$ is invariant during loading. It then represents the distribution of fracture origins (assuming the strength degrading defects are randomly distributed in position and orientation). $P(x)$ will not be invariant for nonlinear bending for which both the length of specimen under stress and the shape of the stress profile change during loading. However, the "risk profile," $P(x)$, calculated for applied stresses typical of those that cause failure will closely approximate the failure origin positions.

Fig. 4 compares the risk profile for the linear and nonlinear bending analyses for $d/a = 1.26$ ($\theta_1 = 60°$), $m = 10$ and the pin/specimen friction coefficient $\mu = 0$. In this case the profiles are not normalized and are a direct evaluation of $f(\sigma)$ so that both the shape and magnitude of failure probability can be compared. As expected, the nonlinear theory predicts that failure is most likely to occur near the center of the specimen while the linear theory gives a uniform probability across the center span. The magnitude of the risk for nonlinear bending is substantially smaller than in linear bending (which is scaled by 10^{-2} in Fig. 4) reflecting the substantially lower stress predicted by this theory.

Fig. 5 shows the normalized risk profile calculated for $d/a = 1.26$ and $m = 10$ for various values of the pin/specimen friction, μ. As friction increases, the likelihood of failure at the pins rises compared to failure near the specimen center. For $\mu = 0.25$ the profile is approximately uniform between the loading pins so that the distribution of failure origins is similar to that predicted by the linear theory. Failure at the pins is undesirable because the stress field there has superimposed upon it the contact stresses between the pin and fiber. The contact stress field will decay over a few fiber diameters. While failure probability becomes localized at the pins at high friction, it will not necessarily be a problem for very thin fibers. However, it is clearly desirable to have a more uniform risk profile and so the friction should preferably be less than ~0.25.

B. Interpretation of Bending Strength

Comparison between the different test methods may be made in two ways: first by calculating the equivalent tensile test length and second by calculating the ratio of strengths measured in four-point bending and other techniques (e.g., tension and two-point bending). However, it is necessary to discuss what is meant by "strength" in this context. In the equivalent analysis for two-point bending [7] mean strengths were compared since, if the tensile strength distribution is assumed to be Weibull, then the two-point bend strength distribution is also Weibull though with a modulus of $m - 1$ instead of m. This meant that the analytic expression for the means of both distributions were readily available. However, for nonlinear four-point bending the distribution is not Weibull if the tensile distribution is Weibull (i.e., the flaw size distribution is an inverse power law [5]), so that the distribution is not known analytically and the mean of the distribution is not readily available. Therefore in the present analysis, ***median*** strengths in tension and bending will be considered. Setting $F(\sigma')$ equal to $1/2$ in (1) yields the condition that $\Re = \ln 2$ for the median strength. In fact the value of ln^2 never explicitly appears in the results since the risk integrals, $\Re_i$, are equated directly to each other with various constraints. Therefore, results are not only valid for median strength but also for any strength percentile. This is not to say that the distributions are therefore identical. For example, if the upper quartile strength were considered, this

is a higher stress than the median giving larger values of d/a at failure and hence different values for the integral in (7).

A second consideration concerns what value is taken for the strength in a particular experiment. Often, the fracture origin is located by examining the broken fragments and the stress at failure is calculated at that position. If the stress distribution is non uniform, as is the case for two- and four-point bending, failure will generally occur away from the point of maximum stress. This means that some region of the specimen survived a higher stress than the calculated failure stress. The failure is therefore conditional on some material being stronger elsewhere; this makes statistical interpretation of the results difficult. This approach to characterizing the strength is useful for characterizing the severity of the flaws that actually cause failure, but it is difficult to extract information on the flaw size distribution. In particular, the measured Weibull modulus of the local stress values is not the same as the Weibull modulus describing the flaw distribution. This approach is not useful for high strength materials because the specimens frequently shatter so that the failure origin cannot be identified. Since one is generally interested in the flaw size distribution, the approach used in this work is to characterize the strength by the overall intensity of the stress field at failure. In two-point bending [7] the intensity was characterized by the peak stress, which in that case occurs at the tip of the bend. While this method could be used here, in part I of this work [1] it is was shown that the maximum stress can occur either at the center ($x = 2a$) or at the loading pins ($x = a, 3a$) depending on the friction and d/a. While part I of this work gives analytic approximations for determining this stress as a function of the pin/specimen friction, it is convenient to avoid the necessity of finding the position of maximum stress for any given situation. For this reason, the intensity of the stress field will be characterized in this work by the stress at the center of the specimen, $x = 2a$, even though at high friction, the stress at the pins can be significantly larger. This choice will have significance when interpreting the results for large friction.

III. Equivalent Tensile Test Length

The equivalent tensile test length is defined as the length of specimen that, when tested in uniaxial tension, gives the same strength as the same material tested in bending. It is therefore a measure of the amount of fiber subjected to significant stress.

When comparing the results of bending and tension, the general approach is to equate the total risk integrals, $\Re_4$ and $\Re_t$, and to apply suitable constraints on the parameters. For the equivalent tensile test length this means the tensile stress, σ, in (12) is equated to the central stress in four-point bending

$$\sigma = \frac{Er}{R_c} \tag{16}$$

where R_c is the radius of curvature at the specimen center $x = 2a$ and solving for the tensile length, l_{eq}, gives

$$l_{\text{eq}} = \frac{G(m)}{\pi} \int_0^{4a} \left(\frac{R_c}{R}\right)^m \frac{dx}{\cos\theta} = \frac{aG(m)}{\pi} \Im \tag{17}$$

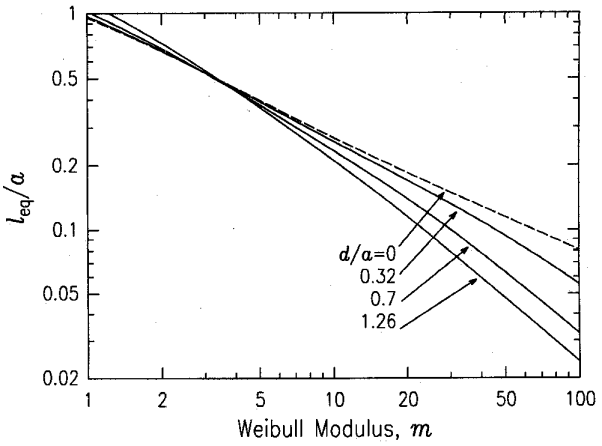

Fig. 6. Normalized equivalent tensile test length as a function of Weibull modulus m calculated for the linear theory ($d/a = 0$), $d/a = 0.32, 0.70$, and 1.26 ($\theta_1 = 20, 40$, and $60°$), and $\mu = 0$.

where

$$\Im = \frac{1}{a} \int_0^{4a} \left(\frac{R_c}{R}\right)^m \frac{dx}{\cos\theta}. \tag{18}$$

The integral in (17) scales with a so that it can be replaced by $a\Im$ where the dimensionless integral, $\Im$, depends on d/a, μ, and m only. While (17) is explicitly independent of the fiber radius, r, it does depend on d/a and the value of d/a at which failure occurs is dependent on both the fiber strength and radius. For the linear bending theory, (17) reduces to

$$l'_{\text{eq}} = \frac{2a}{\pi} G(m) \left(\frac{m+2}{m+1}\right). \tag{19}$$

Fig. 6 shows the equivalent tensile test length, normalized to a, as a function of Weibull modulus for three values of d/a (i.e., three different fiber strengths) as well as the linear theory (the limit of $d/a = 0$). There are two effects which explain the difference between the linear and nonlinear theories. First, the stress peaks at the center of the specimen according to the nonlinear theory but is uniform across the center span for the linear theory. Therefore, the length of fiber subjected to a significant stress is smaller according to the nonlinear theory; especially when the stress is raised to the mth power (e.g., see Fig. 4). Therefore, at high values of m the equivalent tensile test length is shorter than predicted by the linear theory. A second effect is that, at large deflection, the length of fiber between the inner pins is considerably larger than $2a$ [note the factor $\cos^{-1}\theta$ in (5)]. There is therefore physically more fiber under test than considered by the linear theory and this effect dominates at small m, giving a large effective test length. For the case of zero friction, as shown in Fig. 6, the effective tensile test length is actually little different from that predicted by the linear theory for reasonable values of m (2 to ~20). While pristine silica fiber can have m values in excess of 100 [8] it is too strong to be tested by this technique.

Using typical values for a relatively weak optical fiber, $r = 62.5$ μm, $a = 10$ mm, $d/a = 1$, $m = 10$, gives a value of $l_{\text{eq}} \simeq 2$ mm. These parameters give $a/R \simeq 0.5$ and the strain to failure ~0.3%. The equivalent tensile test length

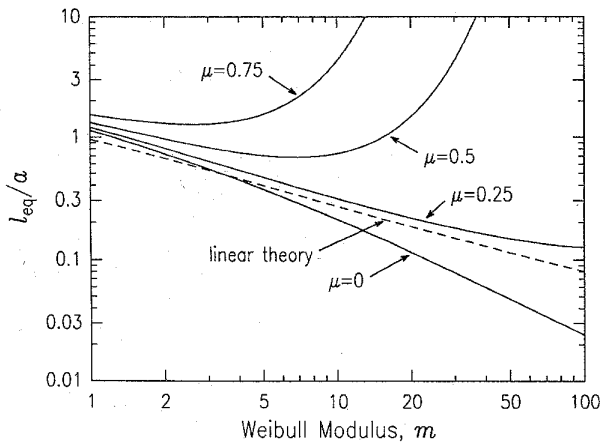

Fig. 7. Normalized equivalent tensile test length as a function of Weibull modulus m calculated for $d/a = 1.26$ and various values of the pin/fiber friction μ.

for a two-point bend experiment on the same fiber is of the same order [7].

Fig. 7 shows the effective tensile test length as a function of Weibull modulus for $d/a = 1.26$ and various values of the pin/specimen friction coefficient, μ. For large values of friction the equivalent tensile test length rises rapidly with m. This is principally due to the calculations characterizing the stress field intensity by the stress at the specimen center rather than at the loading pins where it is higher. Interestingly for $\mu = 0.25$, the results are close to those predicted by the linear bending theory and this is because of the relatively uniform risk profile between the loading pins (Fig. 5).

A. Cylindrical Specimen, Volume Flaws

For defects uniformly distributed throughout the material volume, the element of volume is given by

$$dV = \rho d\rho d\phi ds \tag{20}$$

where ρ is the radial distance of the element from the center of the fiber. The volume flaw equivalent of (5) becomes

$$\Re_{4,V} = \int_{x=0}^{4a}\int_{\phi=0}^{\pi}\int_{\rho=0}^{r}\left(\frac{E\rho\sin\phi}{R\sigma_0}\right)^m \frac{\rho d\rho d\phi dx}{V_0\cos\theta} \tag{21}$$

and the equivalent of (12) becomes

$$\Re_{t,V} = \left(\frac{\sigma}{\sigma_0}\right)^m \frac{\pi r^2 l}{V_0} \tag{22}$$

where the subscript "V" refers to volume flaws. It may readily be shown that the equivalent tensile test length for volume flaws in a fiber is simply related to the value for surface flaws by

$$l_{eq,V} = \frac{2}{m+2} l_{eq}. \tag{23}$$

The results of Figs. 6 and 7 may then be used for volume flaws by applying the simple scaling factor implied by (23).

B. Rectangular Beams

For the case of a rectangular beam with surface defects, of thickness t and width w, it will be assumed that $t \ll w$ so that the probability of failure from the beam edges is negligible. In this case the equivalent tensile test length can be shown to be

$$l_{eq,R} = \frac{1}{2}\int_0^{4a}\left(\frac{R_c}{R}\right)^m \frac{dx}{\cos\theta} = \frac{\pi}{2G(m)} l_{eq} \tag{24}$$

where the subscript "R" refers to the rectangular section. Again, Figs. 6 and 7 can be used to determine the equivalent tensile test length for this geometry by scaling by $\pi/2G(m)$.

For a rectangular beam with volume flaws the above analysis can be readily extended to give the equivalent tensile test length in this case as

$$l_{eq,R,V} = \frac{t}{2w(m+1)} l_{eq,R}. \tag{25}$$

To summarize, the equivalent tensile test length for different types of specimen geometry and flaw distribution can be conveniently calculated from the results for cylindrical specimens with surface flaws by applying simple scaling factors that depend only on the flaw distribution Weibull modulus, m.

IV. Strength Ratio, Four-Point Bending to Tension

The ratio of median strength in tensile and four-point bending is calculated, as for the effective tensile test length, by equating the total risk integrals, (7) and (12). In this case, however, the strength ratio is calculated assuming a fixed tensile test length, l_t. Equations (7), (12), and (17) then give the ratio as

$$\frac{\sigma_4}{\sigma_t} = \left(\frac{l_t}{l_{eq}}\right)^{1/m}. \tag{26}$$

Fig. 8 shows the strength ratio as a function of Weibull modulus, m, for values of $d/a = 0$ (the linear theory) and $d/a = 0.32, 0.7$, and$1.26\,(\theta_1 = 20, 40$, and $60°)$, $\mu = 0$ and for $l_t/a = 1$. There is little dependence on the ratio of d/a, since the dependence shown in Fig. 6 is raised to the mth root (26). The strength ratio is close to unity for these parameters, principally because the tensile test length, l_t, is chosen for convenience to be the pin spacing, a, to calculate the results of Fig. 8. In practice, l_t will be one or two orders of magnitude greater than a with $a \sim 10$ mm and $l_t \sim 0.1$ to 1 m. Under these conditions, the strength ratio may be substantially greater than unity and will show considerably more variation with the Weibull modulus. The ratio of strength of tensile specimens of length l_t and a can be calculated from the well known result of weakest link theory

$$\frac{\sigma(l = l_t)}{\sigma(l = a)} = \left(\frac{a}{l_t}\right)^{1/m}. \tag{27}$$

Thus Fig. 8 can be used to calculate the four-point bend to tensile strength ratio for any tensile test length by modifying results read from the graph by the factor in (27).

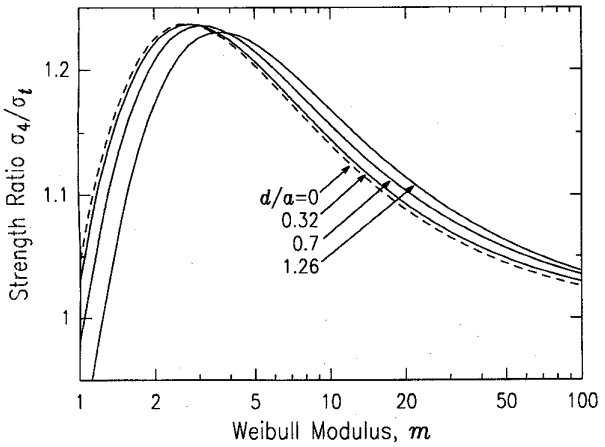

Fig. 8. Ratio of the strengths in tension and four-point bending as a function of the Weibull modulus, m, for various values of d/a, $\mu = 0$, and for the tensile test length of $l_t/a = 1$.

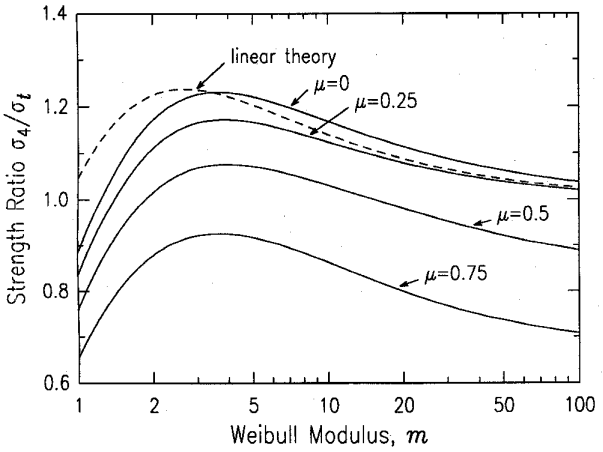

Fig. 9. Ratio of strengths in tension and four-point bending as a function of the Weibull modulus m for $d/a = 1.26$, $l_t/a = 1$ and various values of the pin/fiber friction μ.

Fig. 9 shows the ratio of strength as a function of the Weibull modulus calculated for different values of the friction μ and for $d/a = 1.26$ and $l_t/a = 1$. The results are sensitive to the friction, particularly when recalculated for $l_t \gg a$. At high friction the strength in four-point bending can appear much lower than in tension but this is an artifact of choosing to characterize the four-point strength by the central stress at $x = 2a$ while the stress near the loading pins is substantially higher for high μ. If measurements are made at large μ, it is advisable to report bending results in terms of the equivalent tensile strength, calculated using Fig. 9, so that the numerical value of the strength more closely matches the strength of the failing flaws. It is again suggested that whenever possible the friction should not exceed 0.25 in order to avoid difficulties with interpretation of the results.

A. Other Specimen Geometries and Flaw Distributions

When considering volume flaws, and/or rectangular section specimens, (26) is still valid provided that the appropriate equivalent tensile test length is substituted for l_{eq}. For example, for rectangular specimens with volume flaws, the strength ratio is

$$\frac{\sigma_{4,R,V}}{\sigma_{t,R,V}} = \left(\frac{l_t}{l_{\text{eq},R,V}}\right)^{1/m} \tag{28}$$

where $l_{\text{eq},R,V}$ is given by (25). The other cases considered above can be similarly determined using (23) and (24). The behavior of all these cases can be deduced from Figs. 8 and 9 using the appropriate scaling factors.

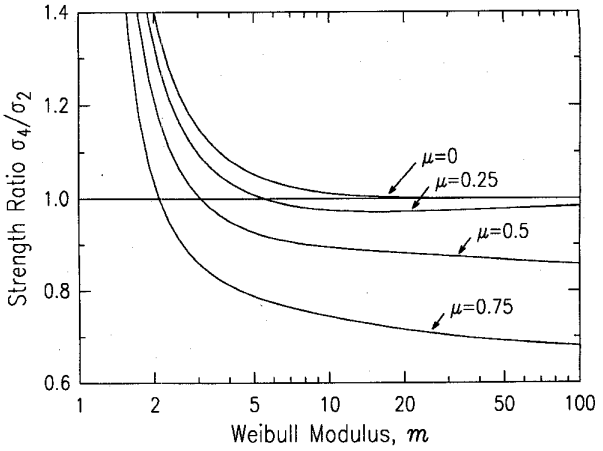

Fig. 10. Ratio of strength in four- and two-point bending calculated for $d/a = 1.26$, $a/R = 200$, and $\sigma_4/E = 0.005$, and for various values of the fiber/pin friction.

V. Strength Ratio, Four- to Two-Point Bending

Normally, it is not possible to test the same specimen in two- and four-point bending since it is either too strong to test in four-point bending or too weak to insert into the two-point bend apparatus. However, when studying fibers over a wide range of strengths both techniques might be required and it is useful to be able to compare them.

The strength ratio in two- and four-point bending can be found by equating (7) and (13) and by setting the four-point strength to the central stress $\sigma_4 = Er/R_c$ and the two-point bend strength to the maximum stress, $\sigma_2 = \sigma_{\max}$, giving

$$\left(\frac{\sigma_2}{\sigma_4}\right)^{m-1} = \frac{\sigma_4}{2E}\frac{1}{r}\int_0^{4a}\left(\frac{R_c}{R}\right)^m \frac{dx}{\cos\theta} G^{-1}\left(\frac{m-1}{2}\right) = \frac{\sigma_4}{2E}\frac{a}{r}\Im G^{-1}\left(\frac{m-1}{2}\right). \tag{29}$$

The ratio σ_4/σ_2 is shown in Fig. 10 calculated for $d/a = 1$, $\sigma_4/E = 0.005$ (0.5% strain to failure) and $a/r = 200$, and for various values of the friction. Except for high friction and very low Weibull modulus, the strength ratio is close to unity. This is not surprising since the geometry of the fiber in four-point bending at high d/a is not dissimilar to that in two-point bending. Statistical considerations play a minor role in comparing two- and four-point bending results.

TABLE I
COMPARISON OF THE RESULTS FOR STRENGTH MEASUREMENT OF 15 SPECIMENS MADE IN BOTH FOUR-POINT BENDING AND TENSION FOR A DELIBERATELY WEAKENED SILICA FIBER

Test Technique	Failure Strain (%)	Standard Error	Weibull Modulus, m	95% Conf. Interval
Four-Point Bending	0.785	0.025	7.9	5.1–11.9
Tension	0.441	0.011	8.8	5.7–13.4

VI. EXPERIMENTAL RESULTS

In order to check the validity of the above statistical comparisons between four-point bend testing and tensile testing, experiments were performed on damaged silica fiber. Damaged silica was chosen rather than inherently weaker fiber so that the ends could be left strong enough to withstand the necessary gripping stresses in tension. 300 μm diameter silica fiber was prepared by stripping in near 200 °C concentrated sulfuric acid and rinsing in deionized water followed by acetone. For the specimens to be tested in tension, a central portion of the fiber measuring 15 cm was stripped leaving the ends coated. Specimens for four-point bend testing were cut to 5 cm lengths and completely stripped. The specimens were then abraded by sliding them through a thick slurry of fine alumina in a consistent fashion (15 strokes). The damaged fiber was then rinsed in deionized water to remove any alumina particles. This produced a uniformly weak fiber within an acceptable strength range for both techniques.

The fiber to be tested in tension was secured by winding the undamaged ends around capstan grips. Since only the damaged portion of the fiber was effectively in test, the gage length was assumed to be 15 cm. A crosshead speed of 11 mm/min was chosen to give a similar strain rate to that of the four-point apparatus ($a = 8$ mm, 500 μm·s^{-1} testing rate) although this was only an approximation as the strain rate is not constant in bending for constant pin speed. Strain results for the tensile specimens were calculated utilizing the measured load at failure and the known Young's modulus for silica (72.2 GPa). Strain results for four-point bend specimens were calculated directly from the displacement d using the correction factor previously described [1]. Both experiments were conducted in ambient laboratory air (~25 °C, 50% humidity); since both experiments used the same loading rate and test environment, the effect of slow crack growth due to environmental moisture is the same for both test methods and so does not influence the comparison of the results.

Table I summarizes the results of breaking 15 specimens for each test method; the Weibull modulus, found by an unbiased maximum likelihood estimator technique [9] is approximately 8 for both test methods. The strength in four-point bending is 1.78 $\pm$ 0.14 (95% confidence) times the tensile strength. Fig. 11 shows the predicted strength ratio, σ_4/σ_t, calculated for the measured d/a of 0.6, $\mu = 0.03$ (the appropriate value for bare silica on steel pins [1]), $a = 7.95$ mm and $l_t = 150$ mm. The experimental value for σ_4/σ_t is also shown with 95% confidence intervals on both the strength ratio and the Weibull modulus. The prediction agrees well with the measured value. While this simple experiment does not in itself verify the statistical analysis presented here for nonlinear bending, since for these parameter values the nonlinear analysis differs little from the linear analysis, the results do show that the modified four-point bend technique does give results that are consistent with tensile testing; both in terms of the mean strength and the scatter in the measured strength.

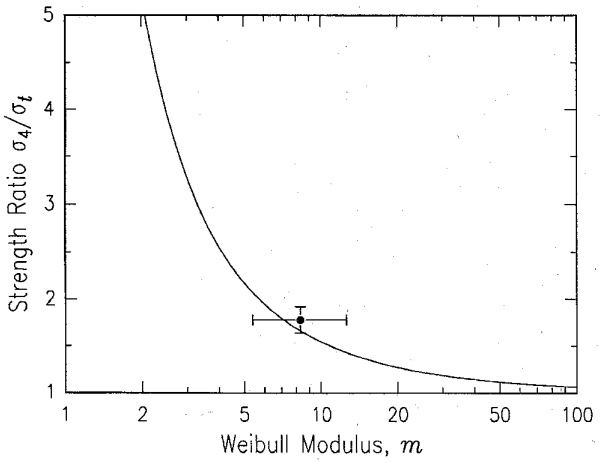

Fig. 11. Comparison of experimental and predicted values of the strength ratio calculated for $d/a = 0.66$, $\mu = 0.03$, and $l_t/a = 18.9$.

VII. DISCUSSION AND CONCLUSION

A detailed statistical analysis of nonlinear four point bending has been developed. The results have been used to compare the four-point bending technique with the two-point bending and tensile techniques by means of the equivalent tensile test length and the strength ratios. In general, even though the nonlinear stress distribution might be quite different from the linear analysis, the statistics of nonlinear bending are similar to those for nonlinear bending except when the pin/specimen friction is high ($\gtrsim$0.25) or the Weibull modulus is small (a broad strength distribution). When the friction is high, there is an undesirable tendency for the specimens to fail at the loading pins rather than in the center of the span. The results of the four-point bending technique are most easily interpreted when the friction is less than 0.25 but this work provides the information necessary to convert the bending strength to an equivalent tensile strength for all reasonable parameter values, including the case of high friction.

While the analysis has been developed for circular section specimens with a uniform distribution of surface flaws, results are also given for rectangular specimens and for volume distributed flaws. The techniques used here are readily extensible to other specimen geometries and flaw distributions.

Experimental results presented here and in the first part of this work [1] show that strength measurements made in four-point bending are consistent with both tensile and two-point bending measurements, both in terms of the strength and the scatter in the strength. Above all, this adaptation of four-point bending has been shown to be a convenient and effective test technique where the weak nature of the specimen prohibits the use of more conventional methods.

REFERENCES

[1] G. J. Nelson, M. J. Matthewson, and B. Lin, "A novel four-point bend test for strength measurement of optical fibers and thin beams: Part I: Bending analysis," see this issue, p. 555–563.
[2] B. Lin, M. J. Matthewson, and G. J. Nelson, "Indentation experiments on silica optical fibers," in *Proc. Soc. Photo-Opt. Instrum. Eng.*, 1990, vol. 1366, pp. 157–166.
[3] G. N. Merberg and J. A. Harrington, "Single-crystal fibers for laser power delivery," in *Proc. Soc. Photo-Opt. Instrum. Eng.*, 1991, vol. 1591, pp. 100–108.
[4] J. J. Colaizzi and M. J. Matthewson, "Mechanical durability of ZBLAN and aluminum fluoride-based optical fiber," *J. Lightwave Technol.*, vol. 12, pp. 1317–1324, 1994.
[5] M. J. Matthewson, "An investigation of the statistics of fracture," in *The Strength of Glass*, C. R. Kurkjian, Ed. New York: Plenum, 1986, pp. 429–442.
[6] P. J. Davis, "Gamma function and related functions," in *Handbook of Mathematical Functions*, M. Abramowitz and I. A. Stegun, Eds. New York: Dover, 1970, pp. 253–293.
[7] M. J. Matthewson, C. R. Kurkjian, and S. T. Gulati, "Strength measurement of optical fibers by bending," *J. Amer. Ceram. Soc.*, vol. 69, pp. 815–821, 1986.
[8] C. R. Kurkjian, J. T. Krause, and U. C. Paek, "Tensile strength characteristics of 'perfect' silica fibers," *J. de Phys.*, vol. 43, pp. C9-585–586, 1982.
[9] D. R. Thoman, L. J. Bain, and C. E. Antle, "Inferences on the parameters of the Weibull distribution," *Technometrics*, vol. 11, pp. 445–460, 1969.

M. John Matthewson, for a photograph and biography, see this issue, p. 563.

Gregory J. Nelson, for a biography, see this issue, p. 563.